



## Crystal structure of $\kappa$ -Ag<sub>2</sub>Mg<sub>5</sub>

Facundo J. Castro<sup>a,b,\*</sup>, Gastón A. Primo<sup>c</sup>, Guillermina Urretavizcaya<sup>a,b</sup>

<sup>a</sup> CNEA, CONICET, Centro Atómico Bariloche, S. C. de Bariloche, Río Negro, Argentina

<sup>b</sup> Universidad Nacional de Cuyo, Instituto Balseiro, S. C. de Bariloche, Río Negro, Argentina

<sup>c</sup> IMBIV-CONICET, Departamento de Química Orgánica, Facultad de Ciencias Químicas, Universidad Nacional de Córdoba, Haya de la Torre y Medina Allende, Edificio de Ciencias II, Ciudad Universitaria, Córdoba, Argentina



### ARTICLE INFO

#### Keywords:

Intermetallics

Structure

Crystal chemistry

X-ray diffraction

Mechanical alloying and milling

### ABSTRACT

The structure of  $\kappa$ -Ag<sub>2</sub>Mg<sub>5</sub> has been refined based on X-ray powder diffraction measurements ( $R_{wp} = 0.083$ ). The compound has been prepared by combining mechanical alloying techniques and thermal treatments. The intermetallic presents the prototypical structure of Co<sub>2</sub>Al<sub>5</sub>, an hexagonal crystal with the symmetries of space group  $P6_3/mmc$ , and belongs to the family of kappa-phase structure compounds. The unit cell dimensions are  $a=8.630(1)$  Å and  $c=8.914(1)$  Å. Five crystallographically independent sites are occupied, Wyckoff positions  $12k$ ,  $6h$  and  $2a$  are filled with Mg, another  $6h$  site is occupied with Ag, and the  $2c$  site presents mixed Ag/Mg occupancy. The crystal chemistry of the structure and bonding are briefly discussed in the paper.

### 1. Introduction

The kappa-phase structure compounds constitute a crystallographic family based on the structure of W<sub>10</sub>Co<sub>3</sub>C<sub>3.4</sub> [1]. These compounds crystallize in the hexagonal system, space group  $P6_3/mmc$ . The metal atom substructure of this prototypical structure is that of Mn<sub>3</sub>Al<sub>10</sub>, and the different kappa-phase structure compounds are obtained by filling the trigonal prismatic ( $2c$ ) or the octahedral ( $6g$ ) interstices of this “host lattice” by p elements or transition metals. If only the trigonal prismatic interstices are filled, the Co<sub>2</sub>Al<sub>5</sub> prototypical structure is obtained. On the other hand, if no more than the octahedral interstices are occupied the Mo<sub>12</sub>Cu<sub>3</sub>Al<sub>11</sub>C<sub>6</sub> structure is obtained. Some compounds have both interstices filled [1].

During an experimental study conducted to analyze MgH<sub>2</sub> destabilization by the formation of Ag-Mg alloys we have identified an intermetallic compound denoted for simplicity Ag<sub>2</sub>Mg<sub>5</sub> that crystallizes with the Co<sub>2</sub>Al<sub>5</sub> structure. Up to now, only eleven compounds with this prototypical structure have been reported [2,3], together with numerous RE<sub>10</sub>TMCD<sub>3</sub> and RE<sub>10</sub>TMAI<sub>3</sub> (RE: rare-earth metal, TM: transition metal) ternary compounds with *anti*-Co<sub>2</sub>Al<sub>5</sub> structure recently identified [4,5]. Interestingly, four of the Co<sub>2</sub>Al<sub>5</sub> structure compounds contain Mg and show some regularity in the periodic table of the elements, namely: Ir<sub>2</sub>Mg<sub>5</sub> [6], Rh<sub>2</sub>Mg<sub>5</sub> [7], Pd<sub>2</sub>Mg<sub>5</sub> [3], and the ternary compound Ir<sub>2.096</sub>Mg<sub>1.980</sub>In<sub>2.924</sub> [3]. The existence of the intermetallic Ag<sub>2</sub>Mg<sub>5</sub> follows this trend. To the best of our knowledge this compound has been only previously mentioned in a PhD thesis [8] and is not included in the Ag-Mg equilibrium phase diagrams [9–11]. We present

here the refinement of its structure, based on X-ray diffraction experiments on powders.

### 2. Experimental and refinement details

The compound was prepared by combining mechanical alloying techniques and thermal treatments. A mixture of magnesium and silver with molar ratio Mg:Ag = 5.25:2 was mechanically alloyed in a planetary mill (Fritsch Monomill Pulverisette 6) under pure argon (99.999%) atmosphere during 10 h. The milling conditions were: 0.5 MPa of argon pressure, ball-to-powder mass ratio equal to 40:1, rotational speed of 400 rpm, and steps of 10 min of milling followed by 10 min of pause. As raw materials Ag nanopowder (< 100 nm, 99.5%, Sigma-Aldrich) and Mg powder obtained from MgH<sub>2</sub> decomposition at 355 °C under vacuum were employed. The hydride used to produce Mg was obtained by milling MgH<sub>2</sub> (hydrogen storage degree, Sigma-Aldrich) under hydrogen (99.999%) during 10 h (similar ball-to-powder mass ratio and milling schedule). The only crystalline phase observed in the as-milled mixture was AgMg (ICDD PDF 65–220) with an approximate composition Ag<sub>0.4</sub>Mg<sub>1.6</sub>. This composition exceeds the equilibrium range of the intermetallic AgMg [9]. However, is usual to obtain non-equilibrium phases by mechanical milling [12]. After a short thermal treatment of 15 h at 350 °C under 0.2 MPa of Ar the compound Ag<sub>2</sub>Mg<sub>5</sub> was observed together with AgMg of approximate composition Ag<sub>0.9</sub>Mg<sub>1.1</sub>, very close to the equilibrium composition of AgMg at 350 °C, according to the phase diagram. This material was further homogenized by a heat treatment at 300 °C under 0.2 MPa of

\* Correspondence to: Centro Atómico Bariloche, Av. Bustillo km 9.5, S. C. de Bariloche, Río Negro, Argentina.  
E-mail address: [fcastro@cab.cnea.gov.ar](mailto:fcastro@cab.cnea.gov.ar) (F.J. Castro).

An atmosphere for 7 days (the temperature has been chosen taking into account that  $\text{Ag}_2\text{Mg}_5$  decomposes around 450 °C [8]). All the materials handling has been done within an Ar filled glovebox with  $\text{O}_2$  and  $\text{H}_2\text{O}$  amounts below 1 ppm.

X-ray diffraction was measured with a Bruker D8 Advance instrument equipped with a PSD detector (LynxEye) and using  $\text{CuK}\alpha$  radiation. An air scatter screen was attached to the instrument to reduce background. The sample was mounted on a low-background Si sample holder. Data were taken in the  $2\theta$  range 10–140° with a 0.010231° step size and a 9 s collection interval. Rietveld refinement of the data was carried out with FullProf [13] using pseudo-Voigt peak-shape functions including an axial divergence asymmetry correction. Sample vertical displacement and micro-absorption effects have been taken into account during the refinement. As individual atomic displacement coefficients could not be reliably refined, only global coefficients were considered. For  $\text{Ag}_2\text{Mg}_5$  the starting structural parameters have been taken from  $\text{Co}_2\text{Al}_5$  [2]. 3D visualization of the structure has been done with VESTA [14].

### 3. Results and discussion

The diffractogram of the homogenized material presents three phases:  $\text{Ag}_2\text{Mg}_5$  (main phase), AgMg and MgO (Fig. 1). This last phase has been formed by reaction of the sample with gaseous impurities during the thermal treatment. Data have been successfully refined including the above mentioned phases. Tables 1 and 2 summarize the main results.

The refinement of the occupancy resulted in single atom full occupancy of the 12k (Mg1), 6h (Ag1), 6h (Mg2) and 2a (Mg4) sites, and mixed Ag/Mg occupancy of the 2c Wyckoff position. The 12k, 6h and 2a sites constitute the metal substructure of the kappa phase structure, whereas the 2c site is the trigonal interstice that can be filled or not, depending on the nature of the atom [1]. In the  $\text{Co}_2\text{Al}_5$  structure this site is fully occupied by Co, but mixed occupancy of this interstice has been observed in  $\text{Pd}_2\text{Mg}_5$  [8].

The coordination polyhedra of the Ag and Mg sites are shown in Fig. 2. The atomic environment of Mg1 is an irregular 14-vertex polyhedron  $\text{Ag}_4\text{Mg}_{10}$ , Ag1 is surrounded by a slightly distorted icosahedron  $\text{Ag}_2\text{Mg}_{10}$ , the coordination polyhedron of Mg2 is a tricapped pentagonal prism  $\text{Ag}_3\text{Mg}_{10}$ , that of the 2c Wyckoff position (Ag2/Mg3) is a tricapped trigonal prism formed by 9 Mg atoms, and finally, Mg4 is surrounded by an icosahedron  $\text{Mg}_6\text{Ag}_6$ . The complete structure can be imagined as columns built by stacking Mg4 icosahedra in the [001] direction. These icosahedra share the triangular faces made of Ag1 atoms and are interconnected by the Ag2/Mg3 tricapped trigonal prisms formed by Mg1 and Mg2 atoms (Fig. 3).

The interatomic distances within the first coordination spheres are

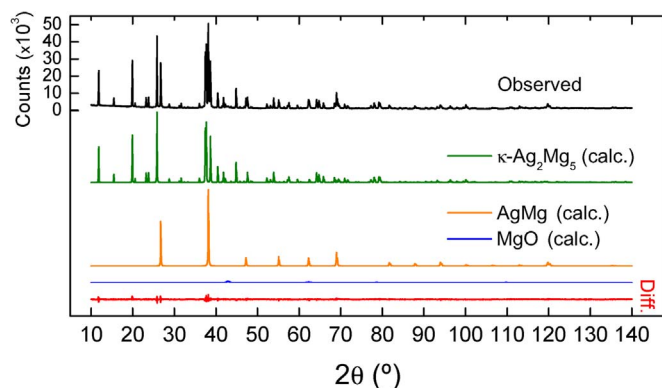


Fig. 1. Observed, calculated and difference X-ray diffraction patterns of the homogenized material.

Table 1

General results of the refinement and crystal structure data for  $\text{Ag}_2\text{Mg}_5$ .

No. of data/parameters	12708/48
$R_{\text{wp}}$	0.083
<b>Phases composition and abundance</b>	
$\text{Ag}_{1.94}\text{Mg}_{5.06}$	65 wt%
$\text{Ag}_{0.93}\text{Mg}_{1.07}$	27 wt%
MgO	8 wt%
<b><math>\text{Ag}_2\text{Mg}_5</math> Crystal data</b>	
Refined composition	$\text{Ag}_{1.945}\text{Mg}_{5.055}$
Z	4
Formula weight	332.7 g mol <sup>-1</sup>
Crystal system	hexagonal
Space group	$P6_3/mmc(n^\circ 194)$
a	8.630(1) Å
c	8.914(1) Å
Volume	0.5749 nm <sup>3</sup>
$\rho_{\text{calc}}$	3.84 g cm <sup>-3</sup>

Table 2

Atomic coordinates for  $\text{Ag}_2\text{Mg}_5$ .

Atom	Wyckoff position	x	y	z	Occup (%)
Mg1	12k	0.2009(5)	2x	0.0517(4)	100
Ag1	6h	0.8829(2)	2x	1/4	100
Mg2	6h	0.538(1)	2x	1/4	100
Ag2/Mg3	2c	1/3	2/3	1/4	89(1)/11(1)
Mg4	2a	0	0	0	100

given in Table 3. In the following we compare these distances with those reported for  $\gamma\text{-AgMg}_4$  [15] and for the isostructural  $\text{Pd}_2\text{Mg}_5$  [3]. The only Ag–Ag pairs in  $\text{Ag}_2\text{Mg}_5$  are Ag1–Ag1, with an interatomic distance of 3.032 Å, similar to the Ag–Ag distance of 2.96 Å reported for  $\gamma\text{-AgMg}_4$  and comparable to the Ag–Ag distance of 2.889 Å for fcc Ag. This suggests significant Ag–Ag interactions in  $\text{Ag}_2\text{Mg}_5$ . On the contrary, the Pd–Pd distance of 3.200 Å for  $\text{Pd}_2\text{Mg}_5$  is considerably greater than Pd–Pd distances in fcc Pd (2.751 Å), indicating weak TM–TM interactions in this compound. Mg–Ag distances in  $\text{Ag}_2\text{Mg}_5$  are in the range 2.65–3.15 Å, a slightly smaller range than 2.70–3.40 Å reported for  $\gamma\text{-AgMg}_4$ . Comparing with Mg–Pd distances in  $\text{Pd}_2\text{Mg}_5$ , 2.60–3.11 Å, the values appear very similar, although Pd is smaller than Ag. Mg–Mg distances in  $\text{Ag}_2\text{Mg}_5$  extend from 3.04 to 3.54 Å, close to the interatomic distances 3.00–3.70 Å for  $\gamma\text{-AgMg}_4$ , and covering a wider range than Mg–Mg distances in  $\text{Pd}_2\text{Mg}_5$ , 2.93–3.25 Å. If we compare these values with the Mg–Mg distance of 3.209 Å in hcp Mg we note that 62% of the Mg–Mg pairs within the first coordination sphere in  $\text{Ag}_2\text{Mg}_5$  have distances greater than 3.209 Å. On the contrary, only 32% of Mg–Mg pairs exceed this value in  $\text{Pd}_2\text{Mg}_5$  suggesting that Mg–Mg bonding is not as important in  $\text{Ag}_2\text{Mg}_5$  as it is in  $\text{Pd}_2\text{Mg}_5$ . Therefore predominant bonding in  $\text{Ag}_2\text{Mg}_5$  is Ag–Ag and Ag–Mg, whereas in  $\text{Pd}_2\text{Mg}_5$  is Pd–Mg and Mg–Mg [3].

An interesting consequence of the characteristics of bonding in  $\text{Ag}_2\text{Mg}_5$  is the greater c/a ratio of this compound compared with that of the isostructural compounds  $\text{Ir}_2\text{Mg}_5$ ,  $\text{Rh}_2\text{Mg}_5$  and  $\text{Pd}_2\text{Mg}_5$  (Table 4). The difference is due to the greater c lattice parameter of  $\text{Ag}_2\text{Mg}_5$ . From the geometry of the structure (Figs. 2 and 3) it can be seen that the magnitude of c depends on the Ag1–Mg4 and Ag1–Ag1 distances. Longer TM1–Mg4 distances and shorter TM1–TM1 distances contribute to greater c lattice parameters. This particular combination takes place in  $\text{Ag}_2\text{Mg}_5$  (Table 4). TM1–Mg4 distances are in all the cases 7–9% shorter than the sum of the corresponding atomic radii but the greater Ag atomic radius produces a longer Ag1–Mg4 distance. On the other hand, the Ag1–Ag1 distance is shorter than the other TM1–TM1 distances and, interestingly, it is only 5% greater than Ag–Ag distance in fcc Ag, whereas Rh1–Rh1 and Pd1–Pd1 distances are 14% and 16%

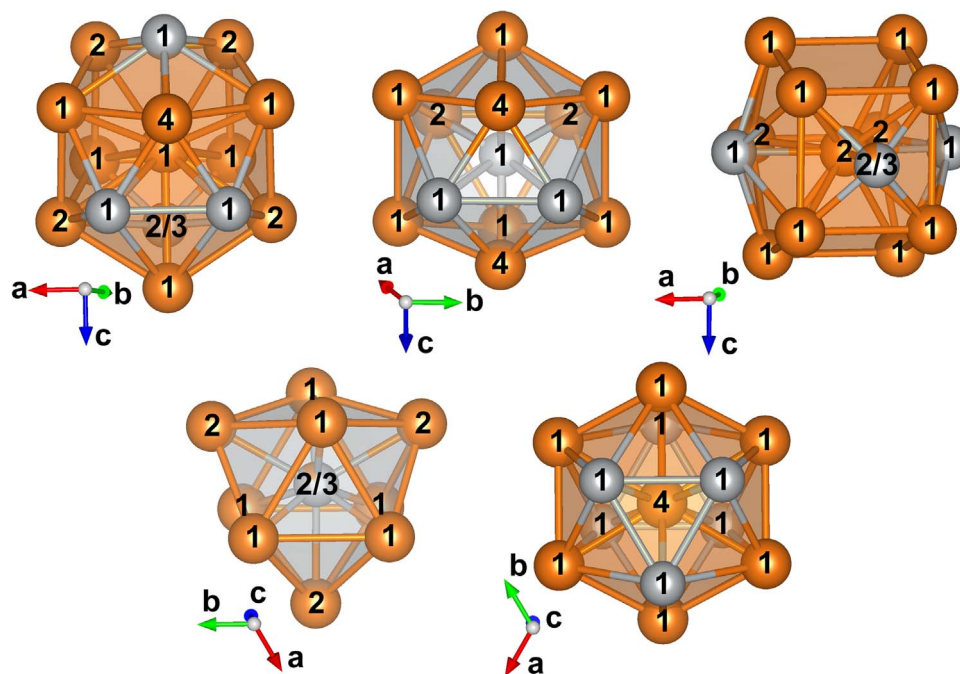


**Fig. 2.** Coordination polyhedra of Mg1 (orange sphere labelled 1), Ag1 (grey sphere labelled 1), Mg2 (orange sphere labelled 2), Ag2/Mg3 (bicolour sphere labelled 2/3) and Mg4 (orange sphere labelled 4).

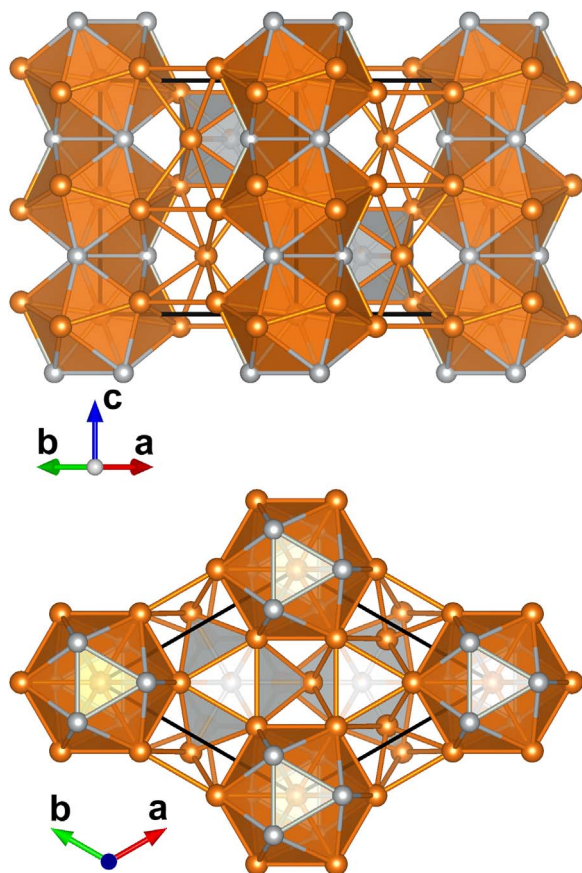


**Fig. 3.** Two views of the complete structure. In orange the coordination polyhedra of Mg4 and in grey the coordination polyhedra of Ag2/Mg3. Black lines represent the unit cell.

**Table 3**

Interatomic distances within the first coordination spheres.

Atom	Coord.	Neighbour	Distance (Å)
Mg1	1	Ag2/Mg3	2.654(8)
	1	Ag1	2.967(4)
	1	Mg4	3.038(3)
	2	Mg1	3.141(4)
	2	Ag1	3.154(5)
	2	Mg2	3.217(5)
	2	Mg2	3.323(5)
	2	Mg1	3.429(8)
	1	Mg1	3.535(6)
	2	Mg2	2.816(9)
Ag1	2	Mg4	2.834(1)
	2	Mg1	2.967(4)
	2	Ag1	3.032(3)
	4	Mg1	3.154(5)
Mg2	2	Ag1	2.816(9)
	1	Ag2/Mg3	3.059(5)
	4	Mg1	3.217(5)
	4	Mg1	3.323(5)
Ag2/Mg3	2	Mg2	3.331(1)
	6	Mg1	2.654(8)
	3	Mg2	3.059(5)
Mg4	6	Ag1	2.834(1)
	6	Mg1	3.038(3)

**Table 4**

Lattice parameters of Mg-containing  $\text{Co}_2\text{Al}_5$ -type compounds and TM1–Mg4 and TM1–TM1 distances. The numbers between parentheses are the sum of the atomic radii of the elements, estimated from the fcc (TM) or hcp (Mg) structures of the pure metals.

Compound	$a$ (Å)	$c$ (Å)	$c/a$	TM1–Mg4 distance (Å)	TM1–TM1 distance (Å)	Ref.
$\text{Ir}_2\text{Mg}_5$	8.601	8.145	0.947	–	–	[6]
$\text{Rh}_2\text{Mg}_5$	8.536	8.025	0.940	2.678 (2.949)	3.073 (2.689)	[7]
$\text{Pd}_2\text{Mg}_5$	8.671	8.164	0.942	2.753 (2.980)	3.200 (2.751)	[3]
$\text{Ag}_2\text{Mg}_5$	8.630	8.914	1.033	2.834 (3.057)	3.032 (2.889)	This work

greater than the corresponding TM1-TM1 distances in the pure TM fcc structure. This suggests again a greater TM–TM interaction in  $\text{Ag}_2\text{Mg}_5$ .

Concerning the stability of  $\kappa\text{-Ag}_2\text{Mg}_5$ , complementary experiments suggest that this phase is a stable low-temperature phase of the Ag-Mg system. In a DSC experiment (not shown here) it was observed that  $\kappa\text{-Ag}_2\text{Mg}_5$  decomposes into AgMg and  $\varepsilon\text{-AgMg}_3$  around 460 °C, but interestingly, if this AgMg and  $\varepsilon\text{-AgMg}_3$  mixture is kept at 250 °C under Ar atmosphere for 6 days,  $\kappa\text{-Ag}_2\text{Mg}_5$  reappears, indicating that the intermetallic is an equilibrium compound. A similar result was reported by Kudla in his Ph.D. dissertation [8]. Detailed thermodynamic studies of the composition of  $\kappa\text{-Ag}_2\text{Mg}_5$  and its stability region in the Ag-Mg phase diagram are currently under way.

### Acknowledgements

The authors gratefully acknowledge fruitful discussions with Dr. J. J. Andrade Gamboa. G. A. Primo also acknowledges the Summer School 2014 from Instituto Balseiro.

### Funding

This work was supported by CONICET [PIP 112 201501 00610]; and Universidad Nacional de Cuyo [06/C486].

### Appendix A. Supporting information

Supplementary data associated with this article can be found in the online version at [doi:10.1016/j.jssc.2017.10.019](https://doi.org/10.1016/j.jssc.2017.10.019).

### References

- [1] A. Härsta, S. Rundqvist, The crystal chemistry of kappa-phases, *J. Solid State Chem.* 70 (1987) 210–218.
- [2] P. Villars, K. Cenzual (Eds.), *Crystal structures of inorganic compounds, Part3, Landolt-Börnstein*, Springer-Verlag, Berlin, 2010.
- [3] V. Hlukhyy, R. Pöttgen, Preparation and structure refinements of  $\text{Pd}_2\text{Mg}_5$  and  $\text{Ir}_{2.096}\text{Mg}_{1.980}\text{In}_{2.924}$  with hexagonal  $\text{Co}_2\text{Al}_5$  type structure, *Intermetallics* 12 (2004) 533–537.
- [4] M. Johnscher, T. Block, R. Pöttgen,  $\text{RE}_{10}\text{Tcd}_3$  ( $\text{RE} = \text{Y, Tb} - \text{Tm, Lu}$ ;  $T = \text{Fe, Co, Ni, Ru, Rh, Pd}$ ) – Rare Earth-rich Phases with Ordered *anti-Co}\_2\text{Al}\_5* Structure, *Z. Anorg. Allg. Chem.* 641 (2015) 369–374.
- [5] C. Benndorf, H. Eckert, O. Janka, Ternary rare-earth aluminium intermetallics  $\text{RE}_{10}\text{TAl}_3$  ( $\text{RE} = \text{Y, Ho, Tm, Lu}$ ;  $T = \text{Fe, Co, Ni, Ru, Rh, Pd, Os, Ir, Pt}$ ) with an ordered *anti-Co}\_2\text{Al}\_5* structure, *Dalton Trans.* 46 (2017) 1083–1092.
- [6] R. Cerný, J.-M. Joubert, H. Kohlmann, K. Yvon,  $\text{Mg}_6\text{Ir}_2\text{H}_{11}$  a new metal hydride containing saddle-like  $[\text{IrH}_4]^{5-}$  and square-pyramidal  $[\text{IrH}_5]^{4-}$  hydrido complexes, *J. Alloy. Compd.* 340 (2002) 180–188.
- [7] R. Ferro, Ricerche sulle leghe dei metalli nobili con gli elementi piu elettropositivi. IV. Le fasi gamma dei sistemi Mg-Rh e Mg-Pd, *Atti della Accademia Nazionale dei Lincei, Classe di Scienze Fisiche, Mat. e Nat., Rend.* 29 (1960) 70–73.
- [8] C. Kudla, Strukturell komplexe intermetallische Phasen Untersuchungen an binären und ternären Phasen der Systeme Ag–Mg und Ag–Ga–Mg Ph.D. Dissertation, Technische Universität Dresden, Dresden, 2007.
- [9] A.A. Nayeb-Hashemi, J.B. Clark, The Ag-Mg System, *Bull. Alloy Phase Diag.* 5 (1984) 348–358.
- [10] H. Okamoto, Ag-Mg, *J. Phase Equil.* 19 (1998) 487.
- [11] C. Dai, D.V. Malakhov, Reoptimization of the Ag-Mg system, *J. Alloy. Compd.* 619 (2015) 20–25.
- [12] C. Suryanarayana, Mechanical alloying and milling, *Prog. Mat. Sci.* 46 (2001) 1–184.
- [13] J. Rodríguez-Carvajal, Recent advances in magnetic structure determination by neutron powder diffraction, *Phys. B – Phys. Cond. Matter* 192 (1993) 55–69.
- [14] K. Momma, F. Izumi, VESTA 3 for three-dimensional visualization of crystal, volumetric and morphology data, *J. Appl. Cryst.* 44 (2011) 1272–1276.
- [15] C. Kudla, Y. Prots, A. Leineweber, G. Kreiner, On the crystal structure of  $\gamma\text{-AgMg}_4$ , *Z. Krist.* 220 (2005) 102–114.